Color Tunable Emission in Ce3+ and Tb3+ Co-doped Ba2Ln(BO3)2Cl (Ln = Gd and Y) Phosphors for White Light-emitting Diodes

ARTICLE *in* SPECTROCHIMICA ACTA PART A MOLECULAR AND BIOMOLECULAR SPECTROSCOPY · AUGUST 2013

Impact Factor: 2.35 · DOI: 10.1016/j.saa.2013.07.076 · Source: PubMed

4 AUTHORS, INCLUDING:

Chongfeng Guo
Northwest University
88 PUBLICATIONS **1,607** CITATIONS

SEE PROFILE

Spectrochimica Acta Part A: Molecular and Biomolecular Spectroscopy 116 (2013) 556–561

Contents lists available at ScienceDirect

Spectrochimica Acta Part A: Molecular and Biomolecular Spectroscopy

journal homepage: www.elsevier.com/locate/saa

Color tunable emission in Ce^{3+} and Tb^{3+} co-doped $Ba_2Ln(BO_3)_2Cl$ (Ln = Gd and Y) phosphors for white light-emitting diodes

Niumiao Zhang [a], Chongfeng Guo [a,*], Heng Jing [a], Jung Hyun Jeong [b,*]

[a] Institute of Photonics & Photon-Technology, National Key Laboratory of Photoelectric Technology and Functional Materials (Culture Base) in Shaanxi Province, National Photoelectric Technology and Functional Materials & Application of Science and Technology International Cooperation Base, Northwest University, Xi'an 710069, China
[b] Department of Physics, Pukyong National University, Busan 608-737, Republic of Korea

HIGHLIGHTS

- Ce^{3+} and Tb^{3+} co-doped chloroborates $Ba_2Ln(BO_3)_2Cl$ (Ln = Y, Gd) green emitting phosphors were prepared.
- Luminescent properties of these phosphors were investigated by comparing methods.
- Energy transfer between Ce^{3+} and Tb^{3+} were discussed in detail.

GRAPHICAL ABSTRACT

PL spectra of (a) $Ba_2Y(BO_3)_2Cl$:0.03Ce^{3+}, $m$$Tb^{3+}$, (b) $Ba_2Gd(BO_3)_2Cl$:0.01Ce^{3+}, $n$$Tb^{3+}$ with different Tb^{3+} contents and (c) the corresponding energy-level diagram. Insets: Dependence of PL intensity of Ce^{3+} and Tb^{3+} on the concentrations of Tb^{3+}.

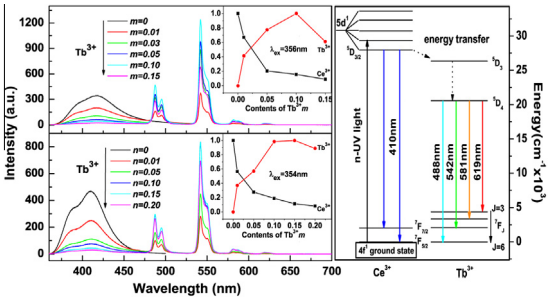

ARTICLE INFO

Article history:
Received 2 May 2013
Received in revised form 13 July 2013
Accepted 25 July 2013
Available online 3 August 2013

Keywords:
Luminescence
Optical property
Phosphor

ABSTRACT

Ce^{3+} and Tb^{3+} co-doped $Ba_2Ln(BO_3)_2Cl$ (Ln = Y and Gd) green emitting phosphors were prepared by solid state reaction in reductive atmosphere. The emission and excitation spectra as well as luminescence decays were investigated, showing the occurrence of efficient energy transfer from Ce^{3+} to Tb^{3+} in this system. The phosphors exhibit both a blue emission from Ce^{3+} and a green emission from Tb^{3+} under near ultraviolet light excitation with 325–375 nm wavelength. Emission colors of phosphors could be tuned from deep blue through cyan to green by adjusting the Tb^{3+} concentrations. The energy transfer efficiency and emission intensity of $Ba_2Y(BO_3)_2Cl$:Ce^{3+}, Tb^{3+} precede those of $Ba_2Gd(BO_3)_2Cl$:Ce^{3+}, Tb^{3+}, and the sample $Ba_2Y(BO_3)_2Cl$:0.03Ce^{3+}, 0.10Tb^{3+} is the best candidate for n-UV LEDs.

Introduction

Recently, white light-emitting diodes (w-LEDs) based upon the combination of blue InGaN chip with yellow phosphors $(A_{1-x}, B_x)_3(C_{1-y}, D_y)_5O_{12}$, where A, B = Y, Gd, Lu, La; C, D = Al, Ga; x and y = 0–1.0 [1], have been used as backlight, flash light, automobile headlamp and so on [2]. These w-LEDs give "cool"-white light with unsatisfactory high correlated color temperature (CCT) over 4000 K and poor color rendering index (Ra) values ranging of 70–80 because of the absence of red component, which cannot meet the requirement to replace the general incandescent and halogen lamps using "warm"-white LEDs with lower CCT and high CRI [3,4]. One of the approaches to overcome the present problems and obtain the w-LEDs with high performance is using near-ultraviolet (n-UV, 350–410 nm) LED chips pumping red, green and blue tricolor phosphors, which provides an excellent color rendering index and the tunable color temperature [5]. However, the range of phosphors suitable for n-UV LEDs is limited. The most frequently

* Corresponding authors. Tel./fax: +86 29 88302661 (C. Guo).
E-mail addresses: guocf@nwu.edu.cn (C. Guo), jhjeong@pknu.ac.kr (J.H. Jeong).

1386-1425/$ - see front matter © 2013 Elsevier B.V. All rights reserved.
http://dx.doi.org/10.1016/j.saa.2013.07.076

used commercial tricolor phosphors for *n*-UV LED are $BaMgAl_{10}O_{17}:Eu^{2+}$ (BAM:Eu^{2+}) for blue, ZnS:Cu^{+}, Al^{3+} for green and $Y_2O_2S:Eu^{3+}$ for red [6]. Unfortunately, the sulfide-based green and red phosphors are inadequate due to their poor stabilities, which seriously decrease the lifetime of the devices [7]. So, it is an urgent task to develop novel green or red phosphors with superior luminescence performances, including long-wavelength excitation and excellent chemical stability.

It is well known that the Tb^{3+} ion is usually used as an activator of green emitting luminescent material due to its predominant $^5D_4 \rightarrow {}^7F_5$ transition peaking at around 545 nm with narrow full width at half maximum (FWHM), leading to excellent color purity and the reproduction quality of optical properties of phosphor. The characteristic sharp emissions of Tb^{3+} are originating from intra-configurational 4*f*–4*f* transitions, which are almost independent of the host lattice because the 4*f* orbital is shielded from the outmost filled $5s^2$ and $5p^6$ orbitals. Tb^{3+} ion can be activated either directly exciting $4f^n$ energy levels or energy transfer process. However, the intensities of Tb^{3+} absorption peaks in the *n*-UV region are very weak and their widths are very narrow due to the strictly forbidden 4*f*–4*f* transitions, which makes it not a perfect activator from the perspective of the application in LEDs. Ce^{3+} ion is a promising sensitizer to enhance the green emission, which can tune the emission color and widen the absorption band of Tb^{3+} due to its strong excitation band and efficient emission band originating from allowed 4*f*–5*d* transition, and has been widely used in many hosts, such as borates, fluorides, sulfides, aluminates, phosphates, and silicates [8–14]. Unfortunately, most of their maximum excitation wavelengths are not over 350 nm, such as 350 nm in $Ca_2Al_3O_6F:Ce^{3+}$, Tb^{3+} [12], 318 nm in $Sr_3In(PO_4)_3:Ce^{3+}/Tb^{3+}$ [13], 335 nm in $Ba_2Gd_2Si_4O_{13}:Ce^{3+}$, Tb^{3+} [14] and 328 nm in $NaCaPO_4:Ce^{3+}$, Tb^{3+} [15]. The maximum excitation wavelength peaked at 400 nm in sulfide-based phosphor $CaLaGa_3S_6O:Ce^{3+}$, Tb^{3+}, but its energy transfer efficiency is very low (about 11%) and the stability is poor [11]. The above results indicate that the above-mentioned phosphors do not match well with the *n*-UV LED chip.

As an important luminescent material host, halo-containing borates have attracted much attention due to their complicated structure, low synthesizing temperature, excellent chemical and physical stability and superior luminescent properties. Rare earth doped these compounds usually exhibit superior luminescent properties, such as Eu^{2+}-doped $M_2B_5O_9Cl$ (M = Sr, Ca) blue emitting [4] and Ca_2BO_3Cl yellow emitting phosphors for *n*-UV LED [16]. Here, we develop a series of new color tunable Ce^{3+} and Tb^{3+} co-doped chloroborates $Ba_2Ln(BO_3)_2Cl$ (Ln = Y, Gd) phosphors, which show intense broad band absorption with maximum excitation at about 355 nm and the tunable emission color from blue to green by adjusting the concentration of activators Tb^{3+}. The results suggest that $Ba_2Ln(BO_3)_2Cl:Ce^{3+}$, Tb^{3+} (Ln = Y, Gd) phosphors could be potential candidates for *n*-UV LEDs.

Experimental

Sample preparation

In $Ba_2Ln(BO_3)_2Cl$ (Ln = Y, Gd) compounds, there are three different cation sites, two different Ba sites and one rare earth ion Yb site. Ba(1) is coordinated by 5O and 4Cl [$Ba(1)O_5Cl_4$], the other Ba(2) is 10-fold with 8O and 2Cl [$Ba(2)O_8Cl_2$], while the Ln^{3+} position is 7 coordinated by oxygen. The ionic radii of the Ba^{2+} ions are 1.47 Å and 1.52 Å in BaO_4Cl_5 and BaO_8Cl_2 polyhedron, and the ionic radii of Gd^{3+} and Y^{3+} are 1.0 Å and 0.96 Å in LnO_7 octahedron, respectively. However, the ionic radii for nine-, and seven-coordinated Ce^{3+} are 1.196 and 1.07 Å, those for Tb^{3+} are 1.095 and 0.98 Å [17]. Therefore, most Ce^{3+}/Tb^{3+} ions prefer to occupy Ln^{3+} sites in the $Ba_2Ln(BO_3)_2Cl$ (Ln = Y, Gd) compounds on the basis of the similar effective ionic radius and valence of the cations. According to our previous results, the optimal contents of Ce^{3+} in $Ba_2Ln(BO_3)_2Cl$ are 3.0% for Ln = Y and 1.0% for Ln = Gd [18]. Here, Ce^{3+}–Tb^{3+} co-doped green emitting phosphors $Ba_2Ln(BO_3)_2Cl$ (Ln = Y, Gd) with fixed optimal Ce^{3+} concentrations were prepared, and their nominal formulas are still named as $Ba_2Y_{0.97-m}(BO_3)_2Cl$:3.0%Ce^{3+}, *m*Tb^{3+} and $Ba_2Gd_{0.99-n}(BO_3)_2Cl$:1.0%$Ce^{3+}$, *n*$Tb^{3+}$. Two series of polycrystalline phosphors were synthesized by traditional high temperature solid state reaction in CO reducing atmosphere. Stoichiometric amount of raw materials containing analytical grade $BaCO_3$, $BaCl_2{\cdot}2H_2O$, H_3BO_3 (excess 5 mol% to compensate for the evaporation and as a flux [19]), and high purity (99.99%) rare earth oxides Gd_2O_3,Y_2O_3, CeO_2, Tb_4O_7 were intimately ground and mixed homogeneously in an agate mortar. The obtained mixture was preheated at 500 °C for 2 h in air. After being cooled to room temperature, the samples were reground and transferred to a small covered alumina crucible, and the small covered crucible was buried in a large corundum crucible with graphite sticks to obtain the Ce^{3+} and Tb^{3+} by reduction. Then, the large crucible with its contents was placed in a muff furnace under ambient atmospheres and fired at 900 °C for 4 h. It was then cooled to room temperature and crushed to fine powder.

Sample characterization

Powder X-ray diffractions (XRD) measurements were performed in the range of $10° \leqq 2\theta \leqq 55°$ using an Rigaku–Dmax 3C powder diffractometer with Cu Kα (λ = 1.5405 Å) radiation. The room temperature photoluminescence (PL) and photoluminescence excitation (PLE) spectra of the phosphors were recorded with a Hitachi F-7000 fluorescence spectrophotometer equipped with a 150 W xenon lamp as the excitation source. The luminescence decay curves of all samples were characterized by an Edinburgh FLS920 combined fluorescence lifetime and steady-state spectrometer. During the measurement process, a 450 W Xe lamp and a 150 W nF 900 ns flash-lamp was used as the excitation source for the luminescence decay curves. To eliminate the second-order emission of the source radiation, a cutoff filter was used in the measurements. Room temperature PL spectra of all samples were tested three times to reduce the error and all measurements were performed at room temperature.

Results and discussion

Structure of sample

XRD is an efficient approach to identify the composition and phase purity of the as-prepared powder sample. Fig. 1 representatively shows the XRD patterns of Ce^{3+} singly and Ce^{3+}–Tb^{3+} doubly doped $Ba_2Ln(BO_3)_2Cl$ (Ln = Y, Gd) phosphors: (a) $Ba_2Y_{0.97}Ce_{0.03}(BO_3)_2Cl$, (b) $Ba_2Y_{0.82}Ce_{0.03}Tb_{0.15}(BO_3)_2Cl$, (c) $Ba_2Gd_{0.99}Ce_{0.01}(BO_3)_2Cl$ and (d) $Ba_2Gd_{0.89}Ce_{0.01}Tb_{0.10}(BO_3)_2Cl$. It is obvious that all the diffraction peaks of the phosphors are in good agreement with those of pure $Ba_2Yb(BO_3)_2Cl$ standard data with JCPDS card No. 79-0967, indicating that the introduction of activators Ce^{3+} or co-doped Ce^{3+}–Tb^{3+} ions were completely dissolved in the hosts and does not generate any impurities or cause any significant changes in the host structures. Results indicate that the obtained phosphors share the same structure with $Ba_2Yb(BO_3)_2Cl$, which crystallizes in a monoclinic structure with the space group $P2_1/m$ [20]. It is also observed that the strongest diffraction peak (013) position at about $2\theta = 29.3°$ shifts to the lower 2θ direction in $Ba_2Gd(BO_3)_2Cl$ host samples (as shown in Fig. 1e) in comparison with XRD patterns of $Ba_2Y(BO_3)_2Cl$ host (Fig. 1a and b), which due to the larger ionic radius of Gd^{3+} than that of Y^{3+}.

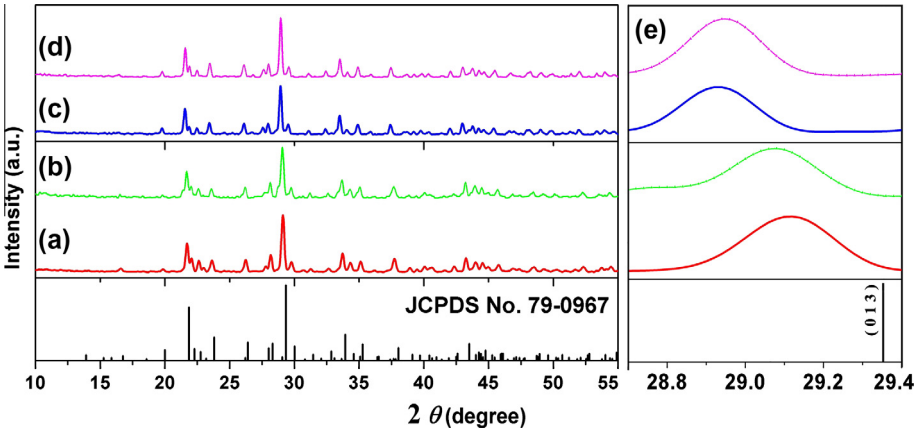

Fig. 1. XRD patterns of samples Ce^{3+}-doped and Ce^{3+}-Tb^{3+} co-doped $Ba_2Y_{0.97}Ce_{0.03}(BO_3)_2Cl$ (a), $Ba_2Y_{0.82}Ce_{0.03}Tb_{0.15}(BO_3)_2Cl$ (b), $Ba_2Gd_{0.99}Ce_{0.01}(BO_3)_2Cl$ (c), $Ba_2Gd_{0.89}Ce_{0.01}Tb_{0.10}(BO_3)_2Cl$ (d), enlarged (013) peaks in the XRD patterns (e) and the standard profile $Ba_2Yb(BO_3)_2Cl$ (JCPDS No. 79-0967) as a reference.

Photoluminescence properties of samples $Ba_2Ln(BO_3)_2Cl:Ce^{3+}/Tb^{3+}$ (Ln = Y, Gd)

PLE and PL spectra of the Ce^{3+}/Tb^{3+} solely- and co-doped samples $Ba_2Ln(BO_3)_2Cl$ (Ln = Gd and Y) are presented in Fig. 2, respectively. Fig. 2a and d shows the PLE and PL spectra of Tb^{3+} solely doped $Ba_2Ln(BO_3)_2Cl$ (Ln = Gd and Y). Monitoring the emission at 542 nm, the PLE spectra of phosphors $Ba_2Ln(BO_3)_2Cl:0.10Tb^{3+}$ (Ln = Gd and Y) include a strong broad band at 260–300 nm and a group of weak sharp lines in the long wavelength region from 300 to 400 nm (insets of Fig. 2a and b). The former should attribute to the spin-allowed $4f^8$–$4f^7 5d$ transition of Tb^{3+}, whereas the latter weak sharp absorption lines are due to the forbidden 4*f*–4*f* transitions of Tb^{3+}. And the intensity of latter is several orders of magnitude weaker than that of the former from the allowed 4*f*–5*d* transition. So the Tb^{3+} ions are difficult to be pumped by the *n*-UV LED chips. Comparing the PLE spectrum of $Ba_2Gd(BO_3)_2Cl:0.10Tb^{3+}$ with that of $Ba_2Y(BO_3)_2Cl:0.10Tb^{3+}$, two sharp lines excitation peaks are found in $Ba_2Gd(BO_3)_2Cl$, a strong sharp line peaked at 273 nm overlap with the Tb^{3+} *f*–*d* excitation band and the other sharp line absorption at 312 nm, which are related to the $^8S_{7/2}$–^6I_J, $^8S_{7/2}$–^6P_J transitions of Gd^{3+} [21]. Meanwhile, the PL spectra of $Ba_2Ln(BO_3)_2Cl:0.10Tb^{3+}$ (Ln = Gd, Y) under the excitation of 273 nm display a series of sharp line emissions at 488, 542, 581 and 620 nm, due to the $^5D_4 \rightarrow {}^7F_J$ (*J* = 6, 5, 4, and 3) characteristic transitions of Tb^{3+} ions, and the green emissions peaked at 542 nm from the $^5D_4 \rightarrow {}^7F_5$ transition dominate the PL spectra. However, no emission in the blue region from the higher energy level $^5D_3$ is observed, which usually be quenched at high Tb^{3+} concentration due to the cross relaxation $^5D_3 + {}^7F_6 \rightarrow {}^5D_4 + {}^7F0$ [22].

As for the Ce^{3+} singly doped samples $Ba_2Ln(BO_3)_2Cl$ (Ln = Gd, Y), the optimal Ce^{3+} concentrations in $Ba_2Gd(BO_3)_2Cl$ and $Ba_2Y(BO_3)_2Cl$ host are 0.01 and 0.03, respectively, which have been investigated in reference 18. Their PL and PLE spectra with optimal compositions are shown in Fig. 2b for Ln = Gd and 2e for Ln = Y. Under the excitation of *n*-UV light with wavelength 354 nm, their PL spectra all exhibit a blue emission with typical unsymmetrical broad band, which corresponds to the transition of Ce^{3+} ions from the $5d^1$ excited state to the $^2F_{5/2}$ and $^2F_{7/2}$ ground states. The PLE spectra monitored at the strongest emission centered at 410 and 417 nm for $Ba_2Gd(BO_3)_2Cl:0.01Ce^{3+}$ and $Ba_2Y(BO_3)_2Cl:0.03Ce^{3+}$ are similar, exhibiting a broad band absorption in *n*-UV region centered at about 354 nm due to the $4f \rightarrow 5d$ transitions of Ce^{3+}. Comparing Fig. 2(b and e) with Fig. 2(a and d), it is observed that

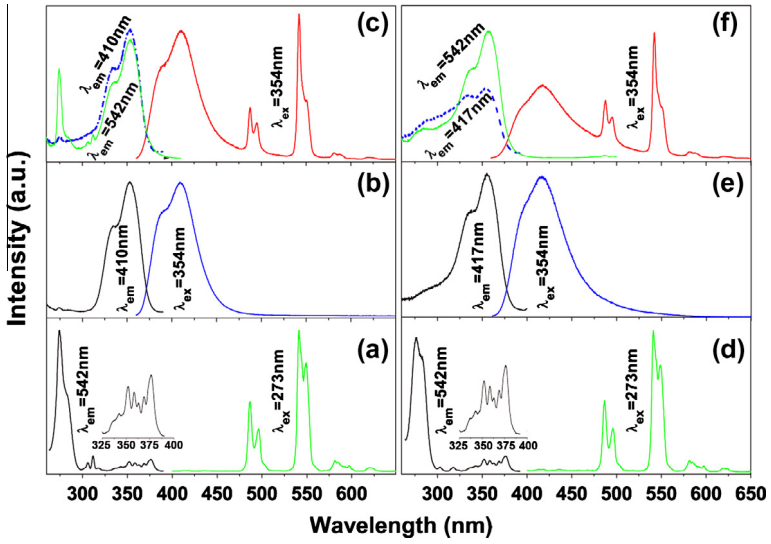

Fig. 2. PLE/PL spectra of Ce^{3+} – Tb^{3+} single- and co-doped samples: (a) $Ba_2Gd(BO_3)_2Cl:0.10Tb^{3+}$, (b) $Ba_2Gd(BO_3)_2Cl:0.01Ce^{3+}$, (c) $Ba_2Gd(BO_3)_2Cl:0.01Ce^{3+}$, $0.10Tb^{3+}$, (d) $Ba_2Y(BO_3)_2Cl:0.10Tb^{3+}$, (e) $Ba_2Y(BO_3)_2Cl:0.03Ce^{3+}$ and (f) $Ba_2Y(BO_3)_2Cl:0.03Ce^{3+}$, $0.10Tb^{3+}$.

there is a small overlap between the emission band of Ce^{3+} and the excitation spectrum of Tb^{3+}, which indicates that the resonance-type energy transfer from Ce^{3+} to Tb^{3+} can be expected to take place in $Ba_2Ln(BO_3)_2Cl$ hosts. Moreover, the exchange interaction energy transfer behavior may also occur, along with the resonant energy transfer, due to the significant overlap between the excitation spectrum of Tb^{3+} and that of Ce^{3+} solely doped $Ba_2Ln(BO_3)_2Cl$ phosphors [23]. It is possible to enhance the absorption intensity in the *n*-UV region and emission intensity of Tb^{3+} by co-doping Ce^{3+} sensitizers to transfer excitation energy to Tb^{3+} ions.

Fig. 2c and f present the PL and PLE spectra of Ce^{3+} and Tb^{3+} co-doped $Ba_2Ln(BO_3)_2Cl$ (Ln = Gd, Y) phosphors. Under the excitation of *n*-UV light with 354 nm wavelength from the characteristic absorption peak of Ce^{3+}, their PL spectra consist of a broad band emission in blue region from the electric-dipole-allowed 4*f*–5*d* transitions of Ce^{3+} and some greatly enhanced sharp line emissions from the electronic transitions within the $4f^7$ configurations of the Tb^{3+}. The PLE spectra monitoring with the Tb^{3+} $^5D_4 \rightarrow {}^7F_5$ (542 nm, solid line) or Ce^{3+} emission (410 nm for Ln = Gd and 417 nm for Ln = Y, dash line) are similar except the relative intensity. Their excitation spectra are all composed of typical broad band absorption from Ce^{3+} in the range of 260–400 nm, which indicates that the efficient energy transfer occurs from Ce^{3+} to Tb^{3+} and makes these phosphors suitable to be excited by *n*-UV LED chips. Whereas, absorptions from Gd^{3+} peaked at 273 and 312 nm are also observed in the PLE spectrum of $Ba_2Gd(BO_3)_2Cl:0.01Ce^{3+}$, $0.10Tb^{3+}$ monitored at 542 nm from Tb^{3+}, which indicates that there exists an energy transfer process from Gd^{3+} to Tb^{3+}.

Fig. 3a and b shows the emission spectra of phosphors $Ba_2Y(BO_3)_2Cl:0.03Ce^{3+}$, mTb^{3+} and $Ba_2Gd(BO_3)_2Cl:0.01Ce^{3+}$, nTb^{3+} as a function of Tb^{3+} concentrations, which were recorded with an excitation wavelength of 354 nm. It can be observed that the emission intensity of Ce^{3+} becomes weaker with increasing Tb^{3+} concentrations although the contents of Ce^{3+} are fixed at 3% and 1% in $Ba_2Y(BO_3)_2Cl$ and $Ba_2Gd(BO_3)_2Cl$, respectively. Whereas, the emission intensity of Tb^{3+} increases gradually with the increase of Tb^{3+} concentrations, and then begin to decline after reaching the maximum at $m = 0.10$ and $n = 0.15$ as a result of concentration quenching. Dependences of PL intensity of Ce^{3+} or Tb^{3+} emission on the concentrations of Tb^{3+} are displayed in the insets of Fig. 3a and b, respectively. Here, the PL intensities are defined as the area under their PL curves calculated by intergrating from 360 to 475 nm

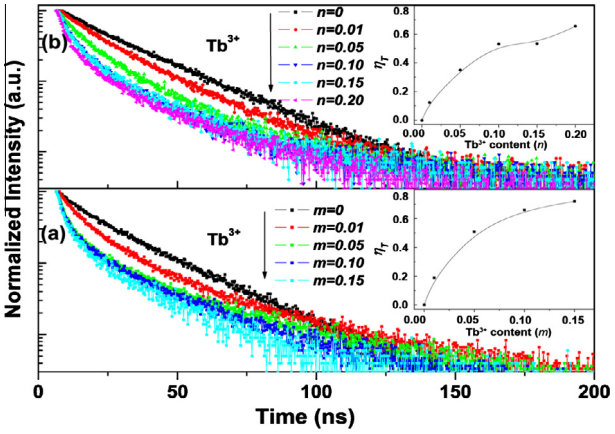

Fig. 4. Decay curves of Ce^{3+} in phosphors (a) $Ba_2Y(BO_3)_2Cl:0.03Ce^{3+}$, mTb^{3+} excited at 354 nm monitored at 417 nm and (b) $Ba_2Gd(BO_3)_2Cl:0.01Ce^{3+}$,$n$Tb^{3+} excited at 354 nm monitored at 410 nm. Insets: Dependence of energy transfer efficiency from Ce^{3+} to Tb^{3+} on the concentrations of Tb^{3+}.

for Ce^{3+} and from 475 to 650 nm for Tb^{3+}, respectively. Comparing Fig. 3a with b, the PL intensity of $Ba_2Y(BO_3)_2Cl:0.03Ce^{3+}$, $0.10Tb^{3+}$ with optimal composition is stronger than that of $Ba_2Gd(BO_3)_2Cl:0.01Ce^{3+}$, $0.15Tb^{3+}$ under the excitation of *n*-UV light with 354 nm wavelength. The above result illuminates that the efficient energy transfer takes place from Ce^{3+} to Tb^{3+} as well as the intensity of blue emission from Ce^{3+} or the green emission from Tb^{3+} could be tuned by appropriately adjusting the concentrations of the sensitizer Ce^{3+} and the activators Tb^{3+}, and the phosphor $Ba_2Y(BO_3)_2Cl:0.03Ce^{3+}$, $0.10Tb^{3+}$ has more potentiality in *n*-UV LED applications.

Based on the analysis of the above spectral results, the corresponding energy levels scheme of $Ba_2Ln(BO_3)_2Cl:Ce^{3+},Tb^{3+}$ (Ln = Gd, Y) with electronic transitions and energy transfer processes is qualitatively displayed in Fig. 3c. Electrons are pumped to the excited 5*d* level from the ground state of Ce^{3+} after absorbing *n*-UV light, then part of the excited state electrons relax to the lowest component $^5D_{3/2}$ energy level of 5*d* level and finally reach to the ground state $^2F_{5/2}$ and $^2F_{7/2}$ of Ce^{3+} by radiative process in the form of broad band blue emissions. Because the value of the energy level of excited 5*d* state of Ce^{3+} is close to that of the $^5D_3$ and other levels

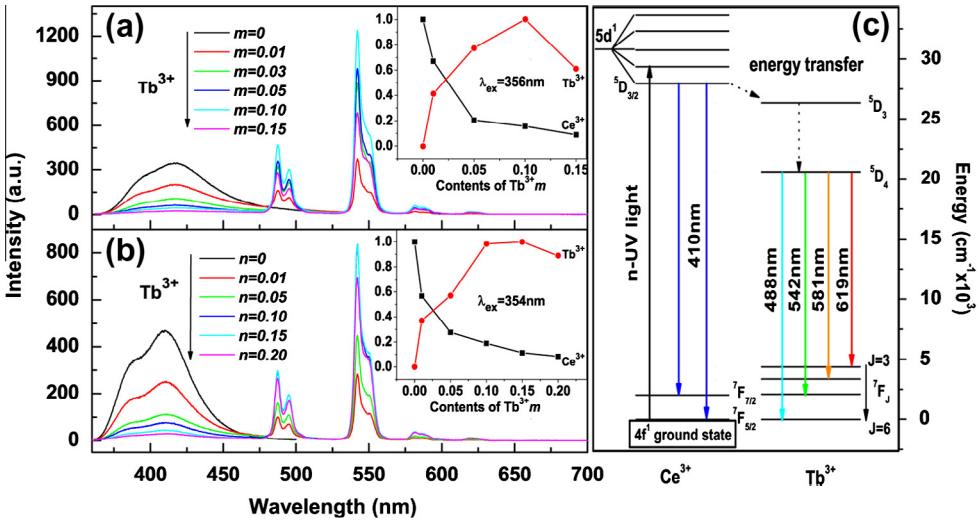

Fig. 3. PL spectra of (a) $Ba_2Y(BO_3)_2Cl:0.03Ce^{3+}$,$m$Tb^{3+}, (b) $Ba_2Gd(BO_3)_2Cl:0.01Ce^{3+}$,$n$Tb^{3+} with different Tb^{3+} contents and (c) the corresponding energy-level diagram. Insets: Dependence of PL intensity of Ce^{3+} and Tb^{3+} on the concentrations of Tb^{3+}.

Table 1
Decay lifetime of $Ba_2Ln(BO_3)_2Cl:Ce^{3+},Tb^{3+}$ excited at 354 nm with the emission monitored at 417 nm for Ln = Y and 410 nm for Ln = Gd. $[\tau^* = (A_1\tau_1^2 + A_2\tau_2^2)/(A_1\tau_1 + A_2\tau_2)]$.

Sample	Tb^{3+} Contents	τ_1	A_1	τ_2	A_2	τ^*	CIE (x, y)
Ln = Y	m = 0	7.52	2722.80	24.54	2544.22	20.3	(0.16, 0.06)
	m = 0.01	6.74	6127.37	28.72	1145.92	16.5	(0.19, 0.24)
	m = 0.05	3.24	17228.81	25.80	909.09	9.9	(0.24, 0.50)
	m = 0.10	2.58	29608.63	21.42	1076.71	6.9	(0.25, 0.54)
	m = 0.15	2.45	11264.40	19.20	342.19	5.7	(0.25, 0.54)
Ln = Gd	n = 0	27.67	2853.99	12.05	1697.60	24.5	(0.17, 0.02)
	n = 0.01	31.52	1275.76	12.60	3652.09	21.4	(0.20, 0.23)
	n = 0.05	26.18	835.21	7.09	3603.74	15.9	(0.21, 0.34)
	n = 0.10	24.54	647.89	4.69	6534.99	11.5	(0.24, 0.51)
	n = 0.15	25.15	319.55	4.36	3620.62	11.4	(0.25, 0.55)
	n = 0.20	22.17	666.79	3.14	12141.90	8.5	(0.25, 0.56)

of Tb^{3+}, it is highly possible that the other part of excited electrons of Ce^{3+} could transfer their energies to Tb^{3+}, promoting the electrons of Tb^{3+} from $^7F_6$ ground state to $^5D_3$ and other excited levels. Then non-radiative relaxation occurred from the high energy levels $^5D_3$ to the $^5D_4$ levels, and Tb^{3+} ions were found to relax by giving several strong sharp line emissions at 488, 542, 581 and 619 nm due to the $^5D_4 \rightarrow {}^7F_6$, $_5D_4 \rightarrow {}^7F_5$, $^5D_4 \rightarrow {}^7F_4$ and $^5D_4 \rightarrow {}^7F_3$ transitions of Tb^{3+} [24]. No emissions from the $^5D_3$ level are observed due to the above mentioned cross-relaxation.

Energy transfer dynamics and luminescence decay

In order to well understand the energy transfer process from Ce^{3+} to Tb^{3+}, the decay curves of Ce^{3+} in $Ba_2Y(BO_3)_2Cl:0.03Ce^{3+}$, mTb^{3+} and $Ba_2Gd(BO_3)_2Cl:0.01Ce^{3+}$, nTb^{3+} phosphors were systemically investigated with excitation at 354 nm and monitored at 417 and 410 nm, respectively. Fig. 4a and b give the decay curves of Ce^{3+} emission in $Ba_2Y(BO_3)_2Cl:0.03Ce^{3+}$, mTb^{3+} and $Ba_2Gd(BO_3)_2Cl:0.01Ce^{3+}$, nTb^{3+}, respectively. For the Ce^{3+} solely doped samples ($m = n = 0$), nearly single exponential luminescence decay curves are observed and the lifetime is about 20.3 and 24.5 ns for $Ba_2Y(BO_3)_2Cl:0.03Ce^{3+}$ and $Ba_2Gd(BO_3)_2Cl:0.01Ce^{3+}$, respectively. However, the decay curves of Ce^{3+} ions significantly deviate from the single exponential rule with the introduction of Tb^{3+} ions, which indicates that the doping of Tb^{3+} ions modifies the fluorescent dynamics of the Ce^{3+} ions [25]. The decay curves could be well fitted with a second-order exponential decay mode by the following equation:

$$I = A_1 \exp(-t/\tau_1) + A_2 \exp(-t/\tau_2) \quad (1)$$

in which I is the luminescence intensity; A_1 and A_2 are constants; t is the time, and τ_1 and τ_2 are rapid and slow lifetimes for exponential components, respectively. The double-exponential decay behaviors of the activators are often observed when the excitation energy is transferred from the donor [26]. The values of A_1, τ_1, A_2 and τ_2 are obtained as shown in Table 1, then the average decay times can be determined by the formula as follows [27,28]:

$$\tau^* = (A_1\tau_1^2 + A_2\tau_2^2)/(A_1\tau_1 + A_2\tau_2) \quad (2)$$

The average decay times τ^* were calculated to be about 16.5, 9.9, 6.9 and 5.7 ns for Ce^{3+} in $Ba_2Y(BO_3)_2Cl:0.03Ce^{3+}$, mTb^{3+} (m = 0.01, 0.05, 0.10 and 0.15), and about 21.4, 15.9, 11.5, 11.4, and 8.5 ns for Ce^{3+} in $Ba_2Gd(BO_3)_2Cl:0.01Ce^{3+}$, nTb^{3+} (n = 0.01, 0.05, 0.10, 0.15 and 0.20), respectively. The lifetime of nanosecond order is one of the specific characteristics of Ce^{3+} doped electric-dipole allowed $5d$–$4f$ transition. It is clearly observed that the average decay times of Ce^{3+} decline rapidly with the increase of Tb^{3+} doping contents, which is attributed to the high efficient energy transfer from Ce^{3+} to Tb^{3+} and also supports the theory that the energy transfer mechanism is non-radiative [29]. On the basis of the above calculated results of the lifetime, the energy transfer efficiency can be estimated using the following equation [25]:

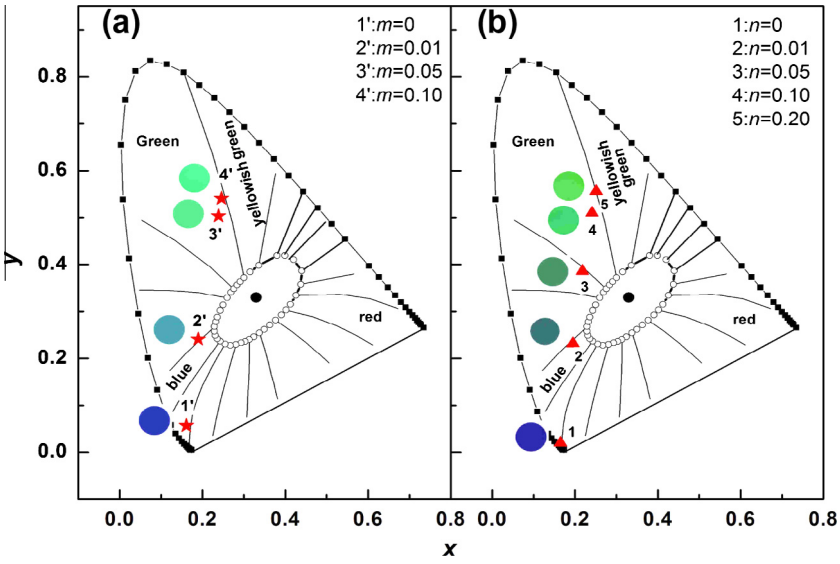

Fig. 5. Representation of the CIE chromaticity coordinates for (a) $Ba_2Y(BO_3)_2Cl:0.03Ce^{3+}$, mTb^{3+} and (b) $Ba_2Gd(BO_3)_2Cl:0.01Ce^{3+}$,$n$Tb^{3+}, respectively.

$$\eta_T = 1 - \frac{\tau_S}{\tau_{S_0}} \quad (3)$$

As a consequence, the dependences of η_T on the concentrations of Tb^{3+} m or n in both series samples are shown in the insets of Fig. 4a and b, respectively. It is observed that the energy transfer efficiency η_T grows swiftly to 66% and 53% with the increase of Tb^{3+} contents in $Ba_2Y(BO_3)_2Cl$:0.03Ce^{3+}, $m$$Tb^{3+}$ and $Ba_2Gd(BO_3)_2$-Cl:0.01Ce^{3+}, $n$$Tb^{3+}$ as $m = n = 0.1$. The values of η_T slowly increase up to72% and 65% with the concentration of Tb^{3+} further increases up to 0.15, which suggests that the energy transfer is close to saturation. The luminescent spectra, decay times of Ce^{3+} and energy transfer efficiency prove that the energy transfer process from Ce^{3+} to Tb^{3+} is efficient in Ce^{3+}–Tb^{3+} co-doped compounds Ba_2-$Ln(BO_3)_2Cl$ (Ln = Gd, Y).

According to the PL spectra upon 354 nm excitation, the CIE chromaticity coordinates for $Ba_2Y(BO_3)_2Cl$:0.03Ce^{3+}, $m$$Tb^{3+}$ and $Ba_2Gd(BO_3)_2Cl$:0.01Ce^{3+}, $n$$Tb^{3+}$ phosphors with different activators contents were calculated and listed in Table 1. Fig. 5a and b shows the CIE chromaticity diagram of two series of samples, respectively. It is found that the values of x and y of the CIE coordinates gradually grow from (0.16, 0.06), (0.17, 0.02) to (0.25, 0.54), (0.25, 0.55) with the increase of Tb^{3+} concentration m from 0 to 0.10 in $Ba_2Y(BO_3)_2Cl$:0.03Ce^{3+}, $m$$Tb^{3+}$ and or n from 0 to 0.15 in Ba_2-$Gd(BO_3)_2Cl$:0.01Ce^{3+}, $n$$Tb^{3+}$, and nearly keep a constant after m or n over 0.10 or 0.15, which indicates that the hue of the phosphor reach saturation. The insets of Fig. 5a and b also present a class of digital photos of the selected phosphors $Ba_2Y(BO_3)_2Cl$:0.03Ce^{3+}, $m$$Tb^{3+}$ and $Ba_2Gd(BO_3)_2Cl$:0.01Ce^{3+}, $n$$Tb^{3+}$ under 365 nm UV lamp excitation. The emission color of samples could be tuned from deep blue through cyan to green with the increase of Tb^{3+} concentrations, which are shown in Fig. 5. On the basis of the above results, the phosphors $Ba_2Y(BO_3)_2Cl$:0.03Ce^{3+}, 0.10Tb^{3+} and $Ba_2Gd(BO_3)_2$-Cl:0.01Ce^{3+}, 0.15Tb^{3+} show the optical compositions, and sample $Ba_2Y(BO_3)_2Cl$:0.03Ce^{3+}, 0.10Tb^{3+} shows the intensest green light. This suggests that $Ba_2Y(BO_3)_2Cl$:0.03Ce^{3+}, 0.10Tb^{3+} can be used as a potential green emitting candidate for n-UV LEDs.

Conclusions

In summary, a class of Ce^{3+} and Tb^{3+} co-doped color tunable $Ba_2Ln(BO_3)_2Cl$ (Ln = Y, Gd) phosphors have been investigated systemically, which exhibits blue emission in the range of 360–475 nm from Ce^{3+} and the enriched green emission spectrum in the region of 475–650 nm from Tb^{3+}. The emission color of the obtained samples can be tuned from deep blue through cyan to green, which depends on the relative concentration of Tb^{3+} and Ce^{3+} because of the different emission compositions of Ce^{3+} and Tb^{3+}. The gradual decreases of the emission intensity and the decay time of Ce^{3+} with the growth of Tb^{3+} concentrations confirm the occurrence of energy transfer from Ce^{3+} to Tb^{3+}. The intense green light from Tb^{3+} could be emitted by a strong broad-band excitation of Ce^{3+} centered at about 354 nm near-UV light, perfectly matching with n-UV LED chips. The phosphor $Ba_2Y(BO_3)_2Cl$:0.03Ce^{3+}, 0.10Tb^{3+} shows the brightest green light and the energy transfer efficiency from Ce^{3+} to Tb^{3+} reaches at 72%. Results indicate that $Ba_2Y(BO_3)_2Cl$:0.03Ce^{3+}, 0.10Tb^{3+} could serve as a potential green emitting phosphor for n-UV LEDs.

Acknowledgements

This work was supported by the high-level talent project of Northwest University, National Natural Science Foundation of China (No. 50802031, 11274251) and Ph.D. Programs Foundation of Ministry of Education of China (No.20070487076), Natural Science Foundation of Hubei Province (2010CDB01607), Technology Foundation for Selected Overseas Chinese Scholar, Ministry of Personnel of China (excellent), Foundation of Key Laboratory of Photoelectric Technology in Shaanxi Province (12JS094), Foundation of Shaanxi Educational Committee (11JK0528) and the Open Foundation of Key Laboratory of Photoelectric Technology and Functional Materials (Culture Base) in Shaanxi Province (ZS11010, ZS12020).

References

[1] J.L. Wu, S.P. Denbaars, V. Srdanov, H. Weinberg, MRS Proc. 667 (2001) G5.1.
[2] C.W. Yeh, W.T. Chen, R.S. Liu, S.F. Hu, H.S. Sheu, J.M. Chen, H.T. Hintzen, J. Am. Chem. Soc. 134 (2012) 14108–14117.
[3] A.A. Setlur, E.V. Radkov, C.S. Henderson, J.H. Her, A.M. Srivastava, N. Karkada, M.S. Kishore, N.P. Kumar, D. Aesram, A. Deshpande, B. Kolodin, L.S. Grigorov, U. Happek, Chem. Mater. 22 (2010) 4076–4082.
[4] C. Guo, Y. Xu, X. Ding, M. Li, J. Yu, Z. Ren, J. Bai, J. Alloys Compd. 509 (2011). L38-L41.
[5] E. Radkov, R. Bompiedi, A.M. Srivastava, A.A. Setlur, C.A. Becker, Proc. SPIE. 5187 (2004) 171–177.
[6] A.K. Cheetham, N. Sharma, US 20050077499A1 [P] April 14, 2005.
[7] C. Guo, F. Gao, Y. Xu, L. Liang, F.G. Shi, B. Yan, J. Phys. D: Appl. Phys. 42 (2009) 095407.
[8] G. Blasse, B.C. Grabmaier, Springer Verlag, Berlin and Heidelberg, 1994. pp. 25.
[9] C. Guo, H. Jing, T. Li, RSC Adv. 2 (2012) 2119–2122.
[10] C. Cao, H.K. Yang, J.W. Chung, B.K. Moon, B.C. Choi, J.H. Jeong, K.H. Kim, J. Mater. Chem. 21 (2011) 10342–10347.
[11] G. Zhang, J. Wang, Y. Chen, Q. Su, Opt. Lett. 35 (2010) 2382–2384.
[12] Z. Xia, R.S. Liu, J. Phys. Chem. C 116 (2012) 15604–15609.
[13] D. Geng, G. Li, M. Shang, D. Yang, Y. Zhang, Z. Cheng, J. Lin, J. Mater. Chem. 22 (2012) 14262–14271.
[14] H. Guo, H. Zhang, J. Li, F. Li, Opt. Exp. 18 (2010) 27257–27262.
[15] N. Guo, Y. Song, H. You, G. Jia, M. Yang, K. Liu, Y. Zheng, Y. Huang, H. Zhang, J. Inorg. Chem. 2010 (2010) 4636–4642.
[16] C. Guo, L. Luan, L. Shi, H.J. Seo, Electrochem. Solid-State Lett. 13 (2010). J28-J31.
[17] C.H. Huang, T.M. Chen, J. Phys. Chem. C 115 (2011) 2349–2355.
[18] W.J. Schipper, G. Blasse, J. Alloys Compd. 203 (1994) 267–269.
[19] R. Shannon, Acta Crystallogr. Sect. A 32 (1976) 751–767.
[20] B. Chu, C. Guo, Q. Su, Mater. Chem. Phys. 84 (2004) 279–283.
[21] P.A.M. Berdowski, M.J.J. Lammers, G. Blasse, J. Chem. Phys. 83 (1985) 476–479.
[22] C. Guo, H. Jing, X. Su, Z. Yang, G. Zhang, J.H. Jeong, J. Mater. Chem. 22 (2012) 13612–13618.
[23] G. Li, S. Lan, L. Li, M. Li, W.W. Bao, H. Zou, X. Xu, S. Gan, J. Alloys Compd. 513 (2012) 145–149.
[24] J. Yang, Y. Su, H. Li, X. Liu, Z. Chen, J. Alloys Compd. 509 (2011) 8008–8012.
[25] N. Guo, Y. Huang, H. You, M. Yang, Y. Song, K. Liu, Y. Zheng, Inorg. Chem. 49 (2010) 10907–10913.
[26] K. Tshabalala, S.H. Cho, J.K. Park, S.S. Pitale, I. Nagpure, R. Kroon, H. Swart, O. Ntwaeaborwa, J. Alloys Compd. 509 (2011) 10115–10120.
[27] S. Buddhudu, M. Morita, S. Murakami, D. Rau, J. Lumin. 83 (84) (1999) 199–203.
[28] C. Peng, Z. Hou, C. Zhang, G. Li, H. Lian, Z. Cheng, J. Lin, Opt. Exp. 18 (2010) 7543–7553.
[29] Y. Chen, J. Wang, X. Zhang, G. Zhang, M. Gong, Q. Su, Sens. Actuators B 148 (2010) 259–263.